CHIN. PHYS. LETT. Vol. 37, No. 6 (2020) 064202

An All-Polarization-Maintaining Multi-Branch Optical Frequency Comb for Highly Sensitive Cavity Ring-Down Spectroscopy *

Kai Ning(宁凯)[1,2], Lei Hou(侯磊)[1,3], Song-Tao Fan(樊松涛)[1,2], Lu-Lu Yan(闫露露)[1,2], Yan-Yan Zhang(张颜艳)[1,2], Bing-Jie Rao(饶冰洁)[1,2], Xiao-Fei Zhang(张晓斐)[1,2], Shou-Gang Zhang(张首刚)[1,2], Hai-Feng Jiang(姜海峰)[1,2]**

[1]*Key Laboratory of Time and Frequency Primary Standards, National Time Service Center, Chinese Academy of Sciences, Xi'an 710600, China*

[2]*School of Astronomy and Space Sciences, University of Chinese Academy of Sciences, Beijing 100049, China*

[3]*Institute of Photonics and Photon-Technology, Northwest University, Xi'an 710069, China*

(Received 7 February 2020)

We demonstrate a multi-branch all polarization-maintaining Er:fiber frequency comb with five application ports for precise measurement of atomic/molecular transition frequencies in the near-infrared region. A fully stabilized Er:fiber frequency comb with a nonlinear amplifying loop mirror is achieved. The in-loop relative instability of stabilized carrier-envelope-offset frequency is 5.6×10^{-18} *at 1 s integration time, while that of the repetition rate is well below* 1.8×10^{-12} *limited by the measurement noise floor of the commercial frequency counter. Five application ports are individually optimized for applications with different wavelengths (1064 nm, 1083 nm, 1380 nm, 1637 nm and 1750 nm). The beat note between the optical frequency comb and continuous laser exhibits the signal-to-noise ratio of at least 30 dB at a resolution bandwidth of 100 kHz. The in-loop frequency instability of the comb is evaluated to be good enough for measurement of rotation-resolved transitions of molecules below 1 kHz resolution.*

PACS: 42.62.Eh, 42.55.Wd, 42.65.Tg DOI: 10.1088/0256-307X/37/6/064202

Optical frequency combs (OFCs) have initiated a new era of time and frequency metrology by transferring the accuracy and stability of an optical reference (e.g., an optical clock system) to other wavelengths of interest.[1] With rapid development, OFCs have found a broad range of applications, including pure microwave generation,[2] astronomical spectrograph calibration,[3] and precision laser frequency spectroscopy.[4] Especially, cavity ring-down spectroscopy (CRDS)[5] is the widely used technique of precision laser frequency spectroscopy. Originally, the combination of CRDS and OFCs with a sub-MHz accuracy was of great interest for a wide range of applications, including absolute positions of several oxygen B-band lines,[6] the derived positions of the absorption lines of four CO isotopologues.[7] Then, Bielska *et al.* reported the unperturbed frequency and collisional shift of the $P7$ line in the O_2 B band with uncertainty of ∼8.5 kHz.[8] Recently, the positions of two ro-vibrational transitions of $^{12}C^{16}O$ at 1.57 μm were determined with an accuracy of ∼0.5 kHz in Ref. [4]. For the sake of completeness, derived line positions of one or more kinds of molecules with highly sensitive CRDS are essential for many investigations in quantum chemistry and molecular physics. However, these applications often require multiple optical frequencies with a performance comparable to the atomic clocks. OFCs provide a means to bridge the gap in frequency between CRDS and optical atomic clocks.

The invention of OFCs has revolutionized the field of measurements of transition frequencies with CRDS. To date, OFCs based on different gain materials have been achieved, such as Ti:sapphire centered at ∼800 nm,[9] Yb:fiber centered at ∼1040 nm[1] and Er:fiber centered at ∼1560 nm.[10] Er:fiber-based OFCs are especially preferred owing to low cost, compactness and maintenance-free operation for the near-infrared (NIR) CRDS.

To date, most representative works include Er:fiber OFCs based on nonlinear polarization rotation (NPR), semiconductor saturable absorber mirror (SESAM) and nonlinear amplifying loop mirror (NALM). Although the most widely used Er:fiber combs by NPR technique to achieve mode-locking with intrinsic low noise,[11] the mode-locking states are sensitive to fluctuations of the temperature, vibration and pressure. Therefore, the performance degradation of OFCs based on NPR fiber lasers is inevitable for long-term operation. Recently, SESAM-based polarization-maintaining (PM) OFCs have been investigated, the advantages of such architectures are self-mode-locking and robust operation. One disadvantage of SESAM-based PM OFCs is that it has higher intrinsic noise than other noise contributions like pump or technical noise.[12] NALM-OFCs with PM fibers are promising candidates for the CRDS measurement, because of their outstanding characteristics compared to other kinds of OFCs, such as low

*Supported by the National Natural Science Foundation of China (Grant Nos. 61825505 and 91536217).

**Corresponding author. Email: haifeng.jiang@ntsc.ac.cn

© 2020 Chinese Physical Society and IOP Publishing Ltd

intrinsic phase noise, self-mode-locking and long-term robust operation.[12,13]

Recently, Er:fiber based PM-NALM-OFCs with three branches or a single port for high-stability comparison of optical lattice clocks have been reported.[14,15] The NALM based all-PM Er:fiber comb with five branches is advantageous for the CRDS measurement, owing to its all-PM architecture that enables long-term robust operation, sufficient output power per mode with optimization for the target frequencies, with relative large distance. In this work, for the purpose of determining the 2^3S–2^3P transition frequency of helium,[16] the $R(0)$–$R(1)$ transition frequency of deuterium,[17] the ${}^{10}F_2 \leftarrow {}^{9}F_1$ transition frequency of methane,[18] and other potential transition frequencies of methane or other molecules,[19] we develop an NALM-based Er:fiber frequency comb with all-PM architecture and five application ports for the CRDS measurement. Every application port is optimized to stabilize corresponding narrow linewidth lasers or external cavity diode lasers (ECDLs). The beat-note between each application port and the corresponding laser exhibits the signal-to-noise ratio of at least 30 dB at a resolution bandwidth of 100 kHz. This system combines with CRDS capable of precise molecular transition frequency measurement with an uncertainty of sub-kilo hertz at target wavelengths (1064 nm, 1083 nm, 1380 nm, 1637 nm and 1750 nm).[4]

A schematic of the system is shown in Fig. 1. The structure of the system consists of two parts, the first part is a self-starting OFC generated by a PM Er:fiber laser with NALM technique, the second part is five application branches for precise atomic/molecular transition frequency measurement.

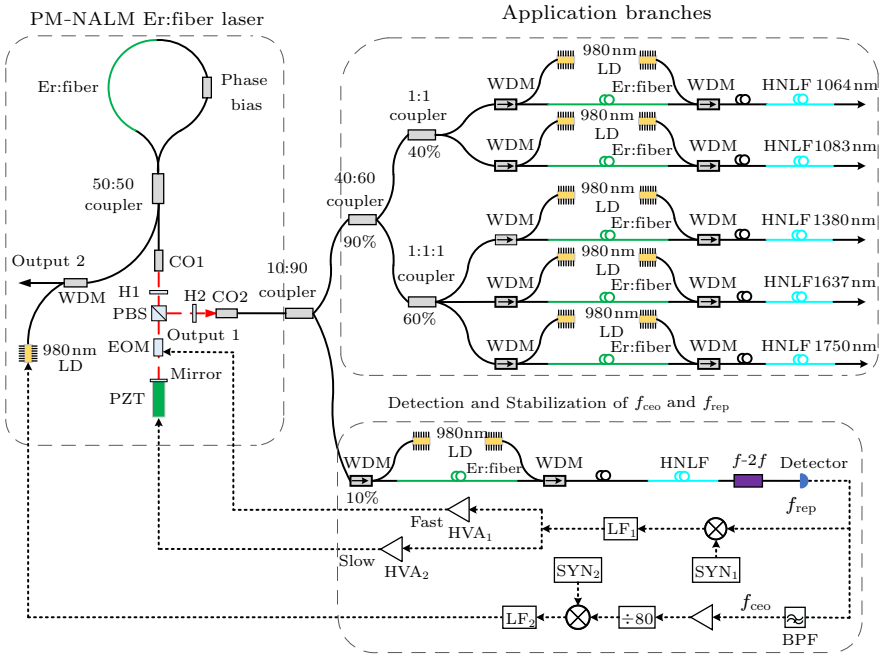

Fig. 1. Schematic of a polarization-maintaining Er:fiber frequency comb and its 5 application branches for precise atomic/molecular transition frequency measurements. LD: laser diode; PZT: piezoelectric transducer; EOM: electro-optic modulator; PBS: polarization beam splitter; H: half-wave plate; CO: collimator; WDM: wavelength division multiplexer; HNLF: highly nonlinear fiber; f–$2f$: f–$2f$ interferometer; BPF: band-pass filter; LF: loop filter; SYN: synthesizer; HVA: high voltage amplifier; f_{rep}: repetition frequency; f_{ceo}: carrier-envelope-offset frequency.

The oscillator (shown in Fig. 1) is a home made PM-NALM Er:fiber laser, which includes a linear cavity in free space and an NALM portion. There is a piezoelectric transducer (PZT) and an electro-optic modulator (EOM) in the linear cavity for slow and fast repetition rate (f_{rep}) stabilizations, respectively. We built the laser with all-PM components, including wavelength division multiplexers with isolators, collimators, couplers, a phase bias module integrated in a micro-optic package, 980 nm laser diodes, Er:fiber and PM1550 fiber. A half-wave plate (H1) was inserted in the linear cavity between the collimator (CO1) and the PBS to adjust the output power. Another half-wave plate (H2) was placed between the PBS and the collimator (CO_2) to adjust the polarization state of output pulses.

To detect the f_{ceo} and implement 5 application branches for CRDS measurement, we distributed the power of output 1 with a 10:90 coupler into 1 mW for f_{ceo} detection and 9 mW for 5 application branches (shown in Fig. 1), since 1 mW is enough to perform f_{ceo} detection and employing multistage amplification may introduce extra phase noise that exceeds the level allowed by the applications, such as a frequency measurement or phase locking.[20]

The f_{ceo} detection portion includes a single stage

bidirectional PM erbium-doped amplifier (EDFA), a PM highly nonlinear fiber (HNLF), an f–$2f$ interferometer (f–$2f$) integrated in a micro-optic package and an InGaAs photodetector (PD) (EOT-3000 A) (shown in Fig. 1). We prechirped seed pulses and obtained broadened pulses with a pulse duration of 1.5 ps in order to reduce the nonlinear effect in the EDFA,[21] then amplified pulses were compressed by a PM1550 fiber. The power of the compressed pulses is ∼280 mW and the pulse duration is ∼88 fs. Ultrashort pulses produced a nonlinear course in the HNLF, making an octave-spanning supercontinuum come true. Finally, $f_{\rm ceo}$ signal from the f–$2f$ interferometer was obtained with an InGaAs PD, meanwhile $f_{\rm rep}$ signal were also detected. The stabilization of $f_{\rm ceo}$ is accomplished by controlling the injection current of the 980 nm pump LD.

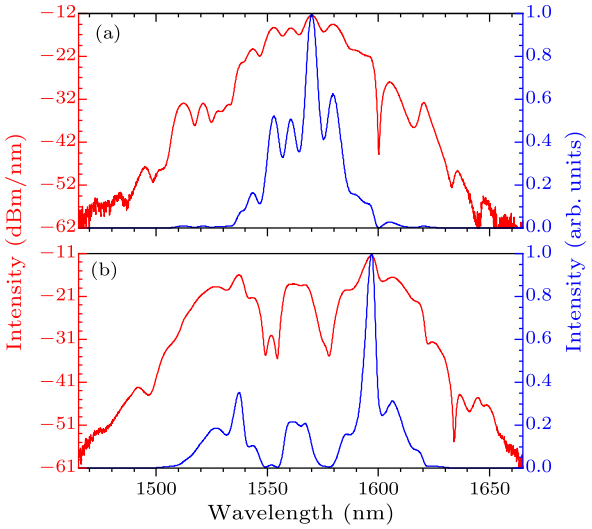

Fig. 2. (a) Measured optical spectra in linear (blue) and log (red) scales from output 1. (b) Measured optical spectra in linear (blue) and log (red) scales from output 2. The vertical axis in the left (red) stands for the intensity of measured laser output spectra in log scales (red), the vertical axis in the right (blue) stands for the normalized intensity of measured laser output spectra in linear scales (blue).

The 5 application branches are custom-made for CRDS measurement, to be exact, two application ports with target wavelengths of 1064 nm and 1083 nm are used to stabilize two corresponding narrow linewidth lasers, which were taken as the reference laser and probe laser in the CRDS measurement. In order to stabilize the length of ring-down (RD) cavity and implement spectrum scanning, the other three application ports with target wavelengths of 1380 nm, 1600 nm and 1750 nm are all used for phase locking with an ECDL independently, which is already locked to an RD cavity. All five application ports mentioned above have a similar structure with the $f_{\rm ceo}$ detection portion, except that there is no f–$2f$ configuration after HNLF. To obtain five application ports with different target wavelengths, we employed different HNLFs in varying length and optimized the injection current of the 980 nm pump LD.

In the experiment, the initiation of mode locking is easily achieved with a 50:50 coupler when pumped at 1095 mW. The average output power of output 1 and output 2 are 10 mW and 6 mW differentially when the oscillator is pumped at a power of 450 mW, the corresponding output spectra are depicted in Figs. 2(a) and 2(b). The full width at half-maximum (FWHM) of output 1 is about 30 nm. The Fourier transform-limited pulse duration is about 84 fs. The output 2 is used to monitor the mode-locking state of the oscillator. The repetition rate of the oscillator is about 136 MHz, and the estimated net cavity dispersion is about $-0.007\,{\rm ps}^2$ at 1550 nm.

To get the $f_{\rm ceo}$, we employed the standard f–$2f$ interference method. The rf spectrum of the $f_{\rm ceo}$ signal is exhibited in Fig. 3(a). The signal-to-noise ratio (SNR) at resolution bandwidth (RBW) of 300 kHz is ∼35 dB, which is adequately high for the home made phase-locking system to stabilize the $f_{\rm ceo}$. A frequency divider ($f/80$) is used to improve the robustness of the $f_{\rm ceo}$ stabilization circuits. Then, the $f_{\rm ceo}$ is phase-locked to a synthesizer (Model SG382) by feeding-back the error signal to a 980 nm pump LD's current control port via a proportional integrator. Figure 3(b) shows the spectrum of the frequency-divided in-loop $f_{\rm ceo}$ after phase-locking with 1 kHz RBW. The control bandwidth of the loop is about 20 kHz.

Moreover, we locked the $f_{\rm rep}$ to 136 MHz of the rf reference signal produced by a synthesizer (Model SG382) with only a low-speed PZT due to the fact that it already meets the demand of the CRDS measurement.[4] Since the frequency instability of OFCs is one of the most important parameters, we measured the in-loop frequency instability of $f_{\rm ceo}$ and $f_{\rm rep}$. Figure 3(c) indicates the in-loop relative frequency instability of $f_{\rm ceo}$ (normalized with the optical frequency of ∼193 THz), which is about 5.56×10^{-18} at 1 s and rolls down to the 10^{-20} level at 10^4 s with a slope of $1/\sqrt{\tau}$. Figure 3(d) shows the in-loop relative frequency instability of $f_{\rm rep}$, which is about 1.8×10^{-12} at 1 s and rolls down to the 10^{-15} level at 10^4 s with a slope of $1/\sqrt{\tau}$. It is basically the same as the noise floor of the measurement system, which is measured by using the same counter to record a 136-MHz reference signal. Therefore, the in-loop $f_{\rm rep}$ frequency stability is limited by the noise floor of the measurement system. To be specific, the measurement of the in-loop $f_{\rm rep}$ signal only reflects the counter noise.[20]

The CRDS measurement usually needs long term phase locking, and we have succeeded in phase-locking $f_{\rm ceo}$ and $f_{\rm rep}$ for more than 1 week. Figures 3(e) and 3(f) present the recorded frequency of phase-locked $f_{\rm ceo}$ and $f_{\rm rep}$ versus time. Standard deviations for $f_{\rm ceo}$ and $f_{\rm rep}$ are estimated to be about 22 mHz, and 67 μHz, respectively.

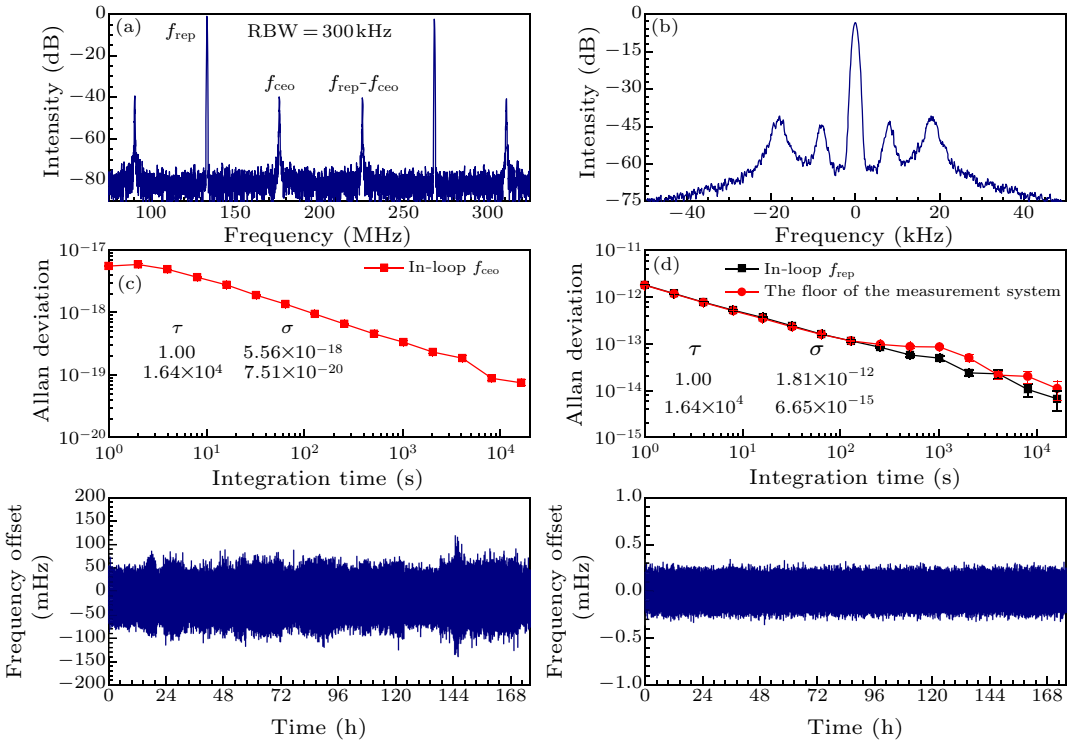

Fig. 3. (a) Measured spectrum from the f–$2f$ interferometer with 300 kHz RBW. (b) Measured spectrum of the frequency-divided in-loop f_{ceo} with 1 kHz RBW. (c) In-loop relative frequency stability of f_{ceo} (solid red square). (d) In-loop relative frequency stability of f_{rep} (solid black square) and the floor of the measurement system (solid red circle). (e) Recorded frequency of phase-locked f_{ceo}. (f) Recorded frequency of phase-locked f_{rep}.

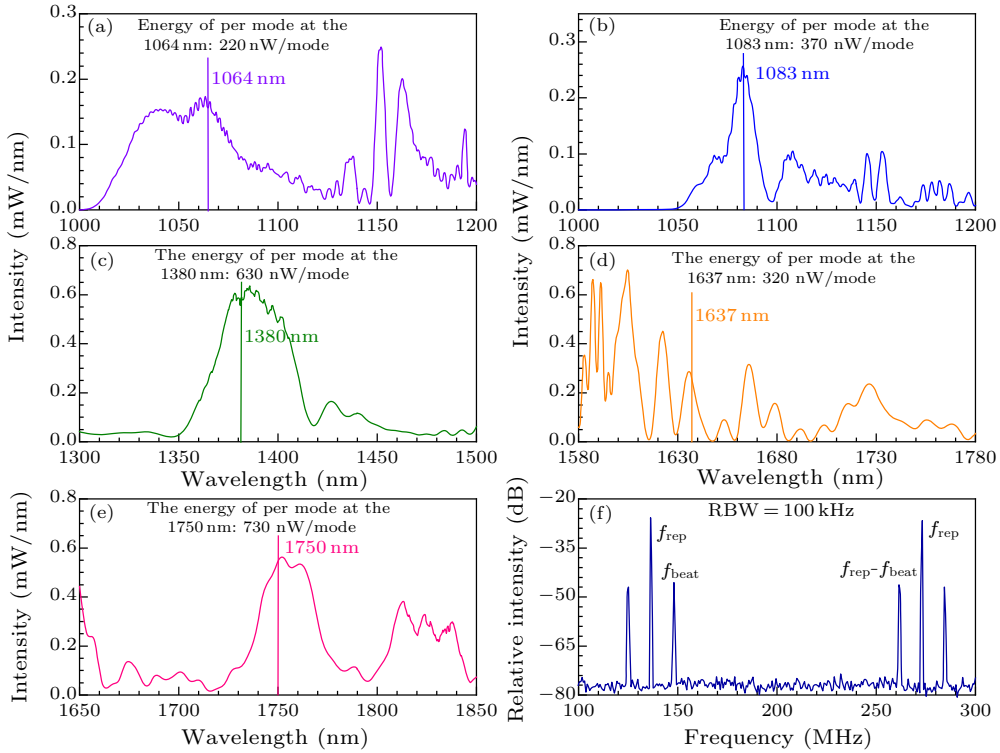

Fig. 4. (a) Observed supercontinuum (SC) spectrum from the 1064 nm application port. (b) Observed SC spectrum from the 1083 nm application port. (c) Observed SC spectrum from the 1380 nm application port. (d) Observed SC spectrum from the 1637 nm application port. (e) Observed SC spectrum from the 1750 nm application port. (f) The frequency spectrum of the beat note between the 1064 nm application port and a narrow linewidth laser with 100 kHz RBW. The vertical lines in (a)–(e) show the target wavelengths.

Figures 4(a)–4(e) show the spectra of the 5 application ports with target wavelengths of 1064 nm, 1083 nm, 1380 nm, 1637 nm and 1750 nm, respectively, in linear scale, which were observed with two optical spectrum analyzers (models AQ6370 and AQ6376, Yokogawa Electric Corp, Tokyo, Japan), and were normalized by thermal-power-detector-measured optical power.

The supercontinuum (SC) structure and energy distribution vary with the utility of different types of HNLF in the case of giving a certain pump source. Especially, the zero dispersion wavelength (ZDW) of HNLFs has an important influence on the SC structure and energy distribution at a given pump source.[22] For the 1064-nm, 1083-nm and 1637-nm ports, we employed a PM-HNLF designated as HNLF1 with the ZDW of 1405 nm and the dispersion slope of $0.026\,\mathrm{ps{\cdot}nm^{-2}km^{-1}}$ at 1550 nm. Due to the larger distance between the ZDW (1405 nm) and the input wavelength (1570 nm), the strong high-order dispersion leads to the energy of solitons transferred to the short-wavelength side and formed a new frequency component,[23] which meets the requirement of the 1064-nm and 1083-nm ports. Meanwhile, as the input pulse power increases, the fission solitons experience a continuous shift to the longer wavelength under the effect of the soliton self-frequency shift,[24–26] which fulfills the need of the 1637-nm port. To generate a much longer wavelength at 1750 nm, we used an HNLF designated as HNLF2 with the ZDW of 1350 nm and the dispersion slope of $0.030\,\mathrm{ps{\cdot}nm^{-2}km^{-1}}$ at 1550 nm, which has similar SC formation process to the HNLF1, and has more energy distributed at longer wavelengths. In order to generate enough spectral components distributed at 1380 nm, we used an HNLF designated as HNLF3 with the ZDW of 1525 nm and the dispersion slope of $0.006\,\mathrm{ps{\cdot}nm^{-2}km^{-1}}$ at 1550 nm. Since the ZDW of HNLF3 is closer to the input light wavelength (1570 nm) and the dispersion slope is small, the spectral components around 1380 nm are abundant, which is in line with Ref. [22].

In addition, we estimated the energy of per mode at five target wavelength regions, which were normalized by thermal-power-detector-measured optical power. The energy of per mode at the 1064-nm, 1083-nm, 1380-nm, 1637-nm and 1750-nm ports are 220, 370, 630, 320, and 730 nW/mode, respectively. Figure 4(f) shows an example of the detected beat signal, which was obtained between the narrow linewidth laser at 1064 nm and the comb modes of the 1064-nm port. The SNR at 100 kHz RBW is about 30 dB. For other ports, we observed enough SNR for frequency stabilization.

In conclusion, we have developed a polarization-maintaining Er:fiber frequency comb with five application branches for precise atomic/molecular transition frequency measurement in the NIR region, the comb based on an all polarization-maintaining Er:fiber laser utilizing a nonlinear amplifying loop mirror. We have confirmed that the frequency stabilized comb and the five application ports are proper functioning during the long-term operation of the CRDS measurement. The polarization-maintaining Er:fiber frequency comb with multi-application branches is convenient and reliable for many applications including frequency comb spectroscopy and lattice clocks.

References

[1] Li Y et al 2017 *Opt. Express* **25** 18017
[2] Rubiola E and Santarelli G 2013 *Nat. Photon.* **7** 269
[3] Chavez Boggio J M et al 2018 *Opt. Commun.* **415** 186
[4] Wang J et al 2018 *J. Chem. Phys.* **148** 029902
[5] O'Keefe A and Deacon D A G 1988 *Rev. Sci. Instrum.* **59** 2544
[6] Domyslawska J et al 2012 *J. Chem. Phys.* **136** 024201
[7] Mondelain D et al 2015 *J. Quant. Spectrosc. Radiat. Transfer* **154** 35
[8] Bielska K et al 2017 *J. Quant. Spectrosc. Radiat. Transfer* **201** 156
[9] Moulton P F 1986 *J. Opt. Soc. Am. B* **3** 125
[10] Diddams S A 2010 *J. Opt. Soc. Am. B* **27** B51
[11] Hofer M, Fermann M E, Haberl F, Ober M H and Schmidt A J 1991 *Opt. Lett.* **16** 502
[12] Hänsel W, Hoogland H, Giunta M, Schmid S, Steinmetz T, Doubek R, Mayer P, Dobner S, Cleff C, Fischer M and Holzwarth R 2017 *Appl. Phys. B* **123** 41
[13] Kuse N, Jiang J, Lee C C, Schibli T R and Fermann M E 2016 *Opt. Express* **24** 3095
[14] Giunta M, Hansel W, Fischer M, Lezius M and Holzwarth R 2017 *Joint Conference of the European Frequency and Time Forum and IEEE International Frequency Control Symposium (EFTF/IFCS)* (Besancon, France, 9–13 July 2017) p 777
[15] Ohmae N, Kuse N, Fermann M E and Katori H 2017 *Appl. Phys. Express* **10** 062503
[16] Zheng X, Sun Y, Chen J J, Jiang W, Pachucki K and Hu S M 2017 *Phys. Rev. Lett.* **119** 263002
[17] Kassi S and Campargue A 2011 *J. Mol. Spectrosc.* **267** 36
[18] Lin H, Lei Y, Feng X and Zhang J T 2019 *Phys. Rev. Lett.* **122** 013002
[19] Arslanov D D, Spunei M, Mandon J, Cristescu S M, Persijn S T and Harren F J M 2013 *Laser & Photon. Rev.* **7** 188
[20] Hisai Y, Akamatsu D, Kobayashi T, Okubo S, Inaba H, Hosaka K, Yasuda M and Hong F L 2019 *Opt. Express* **27** 6404
[21] Zhang Y Y, Yan L L, Zhao W Y, Meng S, Fan S T, Zhang L, Guo W G, Zhang S G and Jiang H F 2015 *Chin. Phys. B* **24** 064209
[22] Fan S T, Zhang Y Y, Yan L L, Guo W G, Zhang S G and Jiang H F 2019 *Chin. Phys. B* **28** 64204
[23] Wai P K A, Menyuk C R, Lee Y C and Chen H H 1986 *Opt. Lett.* **11** 464
[24] Husakou A V and Herrmann J 2001 *Phys. Rev. Lett.* **87** 203901
[25] Husakou A V and Herrmann J 2002 *J. Opt. Soc. Am. B* **19** 2171
[26] Ortigosa-Blanch A, Knight J C and Russell P S J 2002 *J. Opt. Soc. Am. B* **19** 2567